Title
Axonal control of the adult neural stem cell niche.

Journal
Cell Stem Cell, 14(4)

Authors
Tong, Cheuk
Chen, Jiadong
Cebrián-Silla, Arantxa
et al.

Publication Date
2014-04-03

DOI
10.1016/j.stem.2014.01.014

Peer reviewed

Published in final edited form as:
Cell Stem Cell. 2014 April 3; 14(4): 500–511. doi:10.1016/j.stem.2014.01.014.

Axonal Control of the Adult Neural Stem Cell Niche

Cheuk Ka Tong[1,2], **Jiadong Chen**[1], **Arantxa Cebrián-Silla**[3], **Zaman Mirzadeh**[5], **Kirsten Obernier**[1], **Cristina D. Guinto**[1], **Laurence H. Tecott**[2,6], **Jose Manuel García-Verdugo**[3,4], **Arnold Kriegstein**[1,2], and **Arturo Alvarez-Buylla**[1,2]

[1]Department of Neurological Surgery and The Eli and Edythe Broad Center of Regeneration Medicine and Stem Cell Research, University of California, San Francisco, CA, 94143, USA

[2]Neuroscience Graduate Program, University of California, San Francisco, CA, 94158, USA

[3]Laboratory of Comparative Neurobiology, Instituto Cavanilles, Universidad de Valencia, CIBERNED, 46980 Valencia, Spain

[4]Unidad mixta de Esclerosis múltiple y neurorregeneración, IIS Hospital La Fe, Valencia 46013, Spain

[5]Department of Neurosurgery, Barrow Neurological Institute, Phoenix, AZ, 85013, USA

[6]Department of Psychiatry, University of California, San Francisco, CA, 94158, USA

SUMMARY

The ventricular-subventricular zone (V-SVZ) is an extensive germinal niche containing neural stem cells (NSC) in the walls of the lateral ventricles of the adult brain. How the adult brain's neural activity influences the behavior of adult NSCs remains largely unknown. We show that serotonergic (5HT) axons originating from a small group of neurons in the raphe form an extensive plexus on most of the ventricular walls. Electron microscopy revealed intimate contacts between 5HT axons and NSCs (B1) or ependymal cells (E1) and these cells were labeled by a transsynaptic viral tracer injected into the raphe. B1 cells express the 5HT receptors 2C and 5A. Electrophysiology showed that activation of these receptors in B1 cells induced small inward currents. Intraventricular infusion of 5HT2C agonist or antagonist increased or decreased V-SVZ proliferation, respectively. These results indicate that supraependymal 5HT axons directly interact with NSCs to regulate neurogenesis via 5HT2C.

INTRODUCTION

Primary precursors or neural stem cells (NSCs) persist in the adult brain in the ventricular-subventricular zone (V-SVZ) on the walls of the lateral ventricles (Fuentealba et al., 2012; Tong et al., 2014). These NSCs produce new neurons that become integrated into functional

Corresponding author: Arturo Alvarez-Buylla, Phone: 415/514-2348, Fax: 415/514-2346, abuylla@stemcell.ucsf.edu.

circuits, raising questions of whether and how neuronal circuits may themselves contribute to the regulation of postnatal NSCs. It has been suggested that multiple neurotransmitter systems influence postnatal NSC and intermediate progenitor functions (Young et al., 2011). However, little is known about the functions or physical interactions among axonal terminals and NSCs or other progenitors in the adult brain.

The V-SVZ contains a large population of NSCs known as B1 cells (Doetsch et al., 1999; Mirzadeh et al., 2008). These primary progenitors give rise to intermediate progenitors (C cells), which generate large numbers of neuroblasts (A cells) (Doetsch et al., 1996; Ponti et al., 2013). These young neurons form chains that migrate tangentially along the rostral migratory stream (RMS) to the olfactory bulb (OB), where they differentiate into mature interneurons primarily in the granular and periglomerular layers (Lledo et al., 2008; Fuentealba et al., 2012). B1 cells have morphological properties and marker expression profiles of astrocytes. B1 cells have a basal process that contacts blood vessels and a small apical process, frequently containing a primary cilium, that anchors B1 cells to the epithelium and allows these cells to contact the ventricular lumen (Mirzadeh et al., 2008; Shen et al., 2008; Tavazoie et al., 2008). This epithelial organization of B1 cells is reminiscent of radial glia, the NSCs of the developing brain (Kriegstein et al., 2009), which serve as progenitors for the B1 cells (Merkle et al., 2004). Yet, a major difference with radial glia is that the apical contact of B1 cells is surrounded by the large apical surfaces of multiciliated ependymal cells (E1 cells), forming structures known as pinwheels (Mirzadeh et al., 2008). Furthermore, B1 cells function as primary progenitors of new neurons within a fully developed synaptically connected brain. Indeed, cross-sections of the ventricular walls of mice, rats, monkeys and humans have revealed the presence of axons containing the monoamine serotonin (5-hydroxytryptamine; 5HT) (Aghajanian et al., 1975; Lorez et al., 1982; Mathew et al., 1999). Intriguingly, these axons are not within the SVZ proper, but are found inside the ventricles on the surface of the ependyma (Mathew et al., 1999). These supraependymal axons are within a region of the adult brain that is devoid of dendrites or other conventional postsynaptic partners. It is not known how extensive the network of supraependymal axons is or how they influence adult neurogenesis.

Here we use new methods to visualize supraependymal 5HT axons and found an unexpectedly extensive plexus covering most of the walls of the lateral ventricle. These axons developed postnatally and originated from a small subset of neurons in the dorsal and median raphe. Intriguingly, the axons criss-crossed pinwheels to form specialized contacts with B1 and E1 cells. Transsynaptic tracing suggests that dorsal raphe neurons communicated directly with B1 and E1 cells. Supraependymal 5HT release increased V-SVZ cell proliferation. Expression analysis, agonist activation, antagonist blockade and whole-cell patch-clamp recordings indicate that 5HT effects on B1 cells were primarily mediated by the 5HT2C receptors. These findings reveal a direct control of adult NSCs by a select group of raphe 5HT neurons.

RESULTS

A Dense Plexus of Supraependymal Axons along the V-SVZ Neurogenic Niche

Previous work using immunocytochemistry or electron microscopy (EM) has shown that long processes identified as axons are present on the ependymal wall (Aghajanian et al., 1975; Lorez et al., 1982; Mathew et al., 1999). We modified the wholemount preparation of the walls of the lateral ventricle (Mirzadeh et al., 2008), to better visualize the organization of supraependymal axons. Antibodies against acetylated tubulin (AcTub) stained, in addition to the long motile cilia of E1 cells and the short primary cilia of B1 cells, long slender processes that were tightly associated with the ventricular surface (Figure 1A). These processes occurred singly or in bundles of 2–5 and varied in thickness from 0.25–0.95 μm. They overlapped each other and coursed around clusters of ependymal cilia. Varicosities (0.35–0.75 μm diameter) were observed along these axons (Figure 1A). Transmission EM (TEM) images of transverse and tangential sections of the ventricular walls revealed dark-core vesicles, typical of monoaminergic cells, and light-core vesicles present predominantly within the varicosities (Figure 2A). Microtubules and mitochondria were also observed (Figure 2A, B). Microvillae along the length of suprapendymal axons appeared to hold the axons in apposition to the ventricular surface (Figure 2B, C). These observations indicate that the walls of the lateral ventricle are densely innervated by thin unmyelinated axons that are tightly bound to the ependymal surface.

Supraependymal Axons originate from the Dorsal and Median Raphe Nuclei

Previous studies have reported that some raphe nuclei neuronal projections into the forebrain (Hornung, 2003) penetrate into the cerebral ventricles (Aghajanian et al., 1975; Dinopoulos et al., 1995; Mathew, 1999). To confirm this observation and pinpoint the origin of axons that contact the V-SVZ apical surface, we injected a retrograde tracer, fluorescent retrobeads, into the lumen of the lateral ventricle (Figure 1B). The retrobeads labeled the ventricular surface and were not transported deeper into the underlying SVZ (Figure 1C). 3 weeks post-injection, the retrobeads were transported retrogradely into the midbrain where they accumulated in a restricted group of neuronal cell bodies in the caudal aspect of the dorsal raphe nucleus (Figure 1D, E). A smaller number of neurons were also labeled in the median raphe (Figure 1D, F). Sagittal sections confirmed these retrograde tracing results (Figure S1). To address the possibility that retrobead uptake in the third and fourth ventricles could have contributed to raphe staining, we injected green retrobeads into the lateral ventricle and red retrobeads into the third ventricle (or vice versa to control for differential retrograde transport). This consistently resulted in singly labeled raphe neurons from the tracer injected into the lateral ventricle (data not shown). To confirm that dorsal raphe neurons project to the V-SVZ apical surface, we injected a very small volume (10 nl) of the anterograde tracer, biotinylated dextran amine (BDA), into the dorsal raphe (Figure 1G–I). Consistent with our retrograde tracing results, we detected BDA in a subpopulation of supraependymal axons (Figure 1J–L). These findings indicate that a subpopulation of raphe 5HT neurons project supraependymal axons onto the walls of the lateral ventricle.

Serotonergic Axons Blanket the Apical Surface of the Lateral Ventricle; a Plexus that forms Postnatally

Out of the 9 groups of 5HT cells (Hornung, 2003), B1 to B9, the above observations indicate that the dorsal (B6 and B7) and median (B8) raphe gives rise to axons in the lateral ventricles. 5HT has been shown to be present in the V-SVZ (Lorez et al., 1982) and it has been suggested that this neurotransmitter may regulate adult neurogenesis (Brezun et al., 1999). However, it is not known if 5HT is uniquely present on supraependymal axons, or how extensive the supraependymal 5HT innervation is on the walls of the lateral ventricle. Counterstaining the V-SVZ whole mounts showed that AcTub+ processes contained 5HT (Figure 2F–I), as well as punctate expression of the 5HT transporter (SERT) along their length (Figure 2J–M). TEM immunogold staining confirmed that 5HT expression was confined to the supraependymal axons (Figure 2D, E). We found no evidence of 5HT axons beneath the ependymal layer or among SVZ cells.

Using confocal microscopy, we mapped the supraependymal 5HT axons spanning the entire lateral wall of the lateral ventricle in adult mice (Figure 3, Movie S1). Particularly striking was the high density of varicosities in both thin and thick supraependymal axons. The axons also formed distinct structures: loops and bulbous endings (Figure 3D), suggesting physical interaction with the cells in the ventricular wall. Interestingly, supraependymal axons coursed in a pattern reminiscent of that observed for cerebrospinal fluid (CSF) flow and neuroblast migration (Sawamoto et al., 2006), especially along the anterio-posterior axis on the dorsal V-SVZ (Figure 3F), and along the dorso-ventral axis immediately posterior to the adhesion point (Figure 3G). To investigate when during development 5HT axons innervate the V-SVZ, we examined V-SVZ whole mounts from mice of various ages. We found that the axons were scarcely present at birth, but rapidly increased between P0 and P10 (Figure S2A, B). Interestingly, the density of supraependymal 5HT axons continued to increase with age up to 14–15 months (Figure S2C–E). Consistent with this postnatal expansion, growth cone-like structures were observed in the neonatal V-SVZ (Figure S2A). These observations indicate that supraependymal axons invade the ventricular surface soon after birth and continue to grow during juvenile and adult life, suggesting a postnatal function.

Supraependymal Axons form Specialized Contacts with B1 and E1 Cells

We next investigated whether supraependymal axons had ultrastructural features of synapses. From EM of enface and transverse sections, we observed that the supraependymal axon varicosities were filled with light and dark-core vesicles (Figure 4A, B). Mitochondria (Figure 2A), the presynaptic marker synaptophysin (Figure 4C–E) and the vesicular glutamate transporter type 3 (vGluT3) were also found in varicosities (Figure 4F–H). These observations suggest that the supraependymal axon varicosities are active sites for vesicle release. Immunostaining for β-catenin and AcTub or adenylyl cyclase III (ACIII) (to reveal apical cell borders of E1 and B1 cells and the pinwheels) and 5HT (to visualize the supraependymal axons) indicate that these processes criss-crossed the centers of pinwheels (Figure 4I–L). Axonal varicosities were frequently observed on pinwheel cores where B1 cells' apical endings reside. We found that in P30 mice, 75.2±2.2% of pinwheel cores and 53.5±4.3% of B1 cells have their apical surface traversed by the axons. These numbers were similar in 14–15 month old mice (71.7±2.2% of pinwheel cores and 60.4±0.9% of B1 cells).

The proportions of pinwheel cores and B1 cells associated with axons were similar between the anterior dorsal, anterior ventral, posterior dorsal and posterior ventral regions of the V-SVZ (data not shown).

TEM demonstrated that the axons made contacts with the apical surface of B1 cells (Figure 4M, N, Figure S3). B1 cells extended microvilli that enwrapped the axonal varicosities (Figure 4O–R). In some of these contacts, electrondense profiles were observed in the axons (Figure 4P, R). However, no postsynaptic-like specializations were observed in the B1 cells. Supraependymal 5HT axons also formed tight contacts with E1 cells (Figure 4S–U). In this case, the contacts included symmetrical electrondense specializations that resembled desmosomes (Figure 4S). In E1 cells, a fragment of endoplasmic reticulum cisterna with ribosomes on the cytoplasmic side was often observed adjacent to the sites of contact (Figure 4T, U). Interestingly, membrane invaginations and clathrin-coated vesicles were observed in B1 cells and in axons close to their site of contact (Figure 4Q, V), suggesting active exchange of materials between the axons and V-SVZ cells.

Transsynaptic-like Transport from Supraependymal Axons into B1 and E1 Cells in the V-SVZ

To determine if supraependymal 5HT axons and B1 or E1 cells establish synaptic-like contacts, the EGFP-expressing vesicular stomatitis virus (VSV) that has been developed to trace neuronal connections *in vivo* (Beier et al., 2011) was injected into the dorsal raphe. Specifically, we used a VSV pseudotyped with glycoprotein from the lymphocytic choriomeningitis virus (LCMV), which spreads transsynaptically in the anterograde direction (Beier et al., 2011). 4 days post-injection (4dpi), EGFP was present in a small group of 5HT neurons in the dorsal raphe (Figure 5A, B). Prominent labeling was also observed in the V-SVZ and along the RMS (Figure 5L, M). We found a number of VSV(LCMV-G)-infected (EGFP+) B1 cells that were glial-fibrillary acidic protein (GFAP) + (Figures 5C–E, S4B, C) and in the center of pinwheels (Figure 5F–H). A number of E1 cells were also EGFP+ (Figure 5I–K) consistent with the observation that supraependymal 5HT axons also establish intimate contacts with these cells. Labeled cells in the RMS were doublecortin (DCX)+, indicating that the virus also made its way into A cells (Figure 5L, M). Since EGFP expression was mostly confined to the dorsal raphe before 4dpi, the anterograde spread of the VSV(LCMV-G) most likely occurred via the supraependymal axons directly onto B1 cells, rather than through multiple synapses. VSV(LCMV-G) spreads rapidly between A cells (Beier et al., 2011), likely through adherens junctions (Lois et al., 1996). This likely explains the labeling of DCX+ cells at 4dpi. Control experiments injecting the virus dorsal to the raphe did not result in labeling of B1 cells or other progenitors in the V-SVZ or RMS (data not shown). These findings further suggest that a select group of neurons in the dorsal raphe extend projections into the lateral ventricles and establish intimate contacts with B1 cells.

Supraependymal Serotonergic Axons Positively Regulate V-SVZ Proliferation via 5HT2C Signaling

How do supraependymal 5HT axons influence adult neurogenesis in the V-SVZ? To address this question, we infused the 5HT-releasing agent fenfluramine (Arrant et al., 2013) into the

lateral ventricle of adult mice (Figure 5N). Numbers of 5-bromo-2'-deoxyuridine (BrdU)-labeled cells and DCX+ neuroblasts significantly increased following 2-day infusion of fenfluramine, as compared to saline-infused controls (Figure 5O, P, S4E–P), suggesting 5HT induced an increase in proliferation and neurogenesis.

To identify which V-SVZ cell types were responsible for 5HT ligand reception, we used the adult GFAP::GFP transgenic mice for V-SVZ microdissection followed by fluorescence-activated cell sorting (FACS) based on GFP, CD24 and EGFR expression (Pastrana et al., 2009). We enriched for B1, C, A and E1 cells (Figure 6A, B), and verified by quantitative RT-PCR that the sorted cells expressed known markers (Figure S5G). As expected, high levels of the autoreceptors 5HT1A and 5HT1B were detected in the dorsal raphe and 5HT2C was expressed in the choroid plexus (Figure S5I). However, among the 12 5HT receptor subtypes tested, only 5HT2C and 5HT5A were expressed in V-SVZ cells (Figure 6C, D).

To evaluate the effect of 5HT on B1 cells, we performed whole-cell recordings on V-SVZ whole mounts dissected from GFAP::GFP mice. B1 cells were identified by their GFP expression (Figure 6E), their long basal process extending from the cell body (Figure 6F), and their linear current-voltage (I–V) relationship (Figure 6G, H) (Lacar et al., 2010). We found that B1 cells exhibited astrocyte-like membrane properties, with hyperpolarized resting membrane potential (−83.3 ± 1.1 mV, n = 40) and low membrane resistance (32.6 ± 3.3 MΩ, n = 40) (Liu X et al., 2006). Application of 5HT induced an inward current in B1 cells; this current was partially blocked by 5HT2C or 5HT5A antagonists (SB206553 and SB699551, respectively) (Figure 6I, J, L). Co-application of 5HT2C and 5HT5A antagonists abolished the 5HT-induced current in B1 cells (Figure 6J, L). Application of 5HT2C agonist (RO-60-0175) also induced an inward current in B1 cells, that was fully blocked by 5HT2C antagonist (SB206553) (Figure 6K, L). In the presence of the gap junction blocker, cabenoxolone (100 μM), B1 cells exhibited similar resting membrane potential (−85.7 ± 1.2 mV, n = 9), but increased membrane resistance (130.6 ± 16.2 MΩ, n = 9) (Lacar et al., 2010), consistent with decreased electrical coupling. A consistent, albeit smaller in amplitude, inward current was recorded upon application of 5HT2C agonist (Figure 6L). 5HT-induced currents in B1 cells were sensitive to Ba2+, a K+ channel blocker (Figure 6L) (Bonsi et al., 2007), suggesting a main contribution of K+ currents to the 5HT response of B1 cells.

The above suggests that 5HT axons could directly regulate B1 cells, possibly affecting their progenitor function through 5HT2C and/or 5HT5A receptors. We therefore tested the effects of 5HT2C agonist and antagonist on V-SVZ proliferation in adult mice (Figure 7A). After 5-day infusion of RO-60-0175 into the lateral ventricle, the number of BrdU+ cells in the V-SVZ increased (Figure 7B, E). Conversely, a 5-day infusion of SB206553 resulted in a decrease in the number of BrdU+ cells (Figure 7D, F).

To better understand the cell population that contributes to the proliferative effect of 5HT2C activation, we analyzed V-SVZ proliferation in GFAP::GFP mice after acute treatment (4 hours) of either the agonist or antagonist of 5HT2C (Figure 7G). The total number of BrdU+ cells was significantly higher in the agonist-injected mice compared to the antagonist-injected mice 4 hours post-injection (Figure S6B). Co-immunostaining for GFAP/GFP (B1

cell marker), Mash1 (C cell marker), DCX (A cell marker) and BrdU in V-SVZ whole mounts (Figure 7H–P) showed no significant difference in the total numbers of B1, C or A cells in agonist- and antagonist-treated mice (Figure S6C–E). The proportion of C and A cells that were BrdU+ was also not significantly different (Figure 7R, S). In contrast, the proportion of B1 cells that were BrdU+ was significantly higher in agonist-injected mice (15.1 ± 2.4%) compared to antagonist-injected mice (7.4 ± 0.6%) (Figure 7Q). These results suggest that B1 cells increased their proliferation in response to 5HT2C activation.

DISCUSSION

We provide evidence for an extensive plexus of supraependymal 5HT axons on the apical surface of the lateral ventricles where they contact B1 and E1 cells with specialized junctions. These axons, which originate from a small group of neurons in the raphe, transfer VSV(LCMV-G) -- used to trace synaptic contacts (Beier et al., 2011) -- to B1 and E1 cells. Characterization of 5HT receptor subtype expression in the V-SVZ cells, electrophysiology recordings, and pharmacological studies, implicate 5HT2C receptors in the 5HT stimulation of adult V-SVZ cell proliferation and neurogenesis.

The presence of axons in the ventricle next to the ependymal lining was first noted by histochemistry for monoamines (Lorez et al., 1982). Elegant neurotoxin experiments suggested that many of these supraependymal axons were serotonergic (Lorez et al., 1982). However, the density and extent of this axonal plexus and its relationship to the V-SVZ neurogenic niche remained unknown. Other work using 5HT staining in coronal or sagittal brain sections, revealed only portions of putative supraependymal axons, as the distribution of 5HT axons was difficult to map in sectioned material. Previous work suggested the existence of an extensive network of 5HT axons within the SVZ (Jahanshahi et al., 2011), an observation that we were not able to confirm. Oblique cutting angles can suggest a subependymal location for supraependymal axons. We therefore adapted the wholemount V-SVZ preparation (Mirzadeh et al., 2008) to map supraependymal 5HT axons. This approach revealed an extensive plexus with large numbers of overlapping axons and varicosities that express presynaptic terminal markers synaptophysin and vGluT3. Wholemount staining also allowed the juxtaposition of supraependymal axons and pinwheels (Mirzadeh et al., 2008).

EM studies revealed intimate contacts between vesicle-filled supraependymal axon varicosities and the small apical processes of a subset of B1 cells. Both dark and light-core vesicles were observed, consistent with prior observations that 5HT may be co-released with other co-transmitters (Fu et al., 2010). A high incidence of membrane invaginations indicative of active exo-endocytosis was observed between supraependymal axon varicosities and both B1 and E1 cells. However, the specialized contacts between the axons and B1 and E1 cells differ significantly from classical synapses between neurons. For example, we did not observe a typical postsynaptic density in B1 cells. Yet the presence of 5HT2C and 5HT5A receptors in B1 cells suggests that these cells have evolved response mechanisms to 5HT. The time-course of B1 cell response to 5HT, as demonstrated by electrophysiology, is much slower than that required for transmission between neurons and therefore may not necessitate complex postsynaptic machinery.

The transfer of VSV(LCMV-G) from dorsal raphe neurons to B1 cells reinforces the concept of material exchange between supraependymal axons and NSCs. While the VSV(LCMV-G) is a known anterograde transsynaptic tracer, it operates by fusing with a closely juxtaposed membrane where there is rapid membrane fusion and recycling (Beier et al., 2011), so it is possible that the VSV(LCMV-G) crossed over from the supraependymal axons to the B1 or E1 cells not by specific synaptic transmission but by close membrane appositions and intimate exo-endocytosis. The expression of EGFP by A cells along the SVZ and RMS might be due to viral infection of their progenitor B1 cells, or A cells themselves might be infected via dorsal raphe projections within these migratory corridors. Based on our observations, it is more likely that EGFP+ DCX+ cells were progeny of VSV(LCMV-G)-infected B1 cells because EGFP+ DCX+ cells were only observed in the caudal RMS proximal to the V-SVZ and we did not observe 5HT axons near the A cells in the SVZ. It is not clear how large numbers of A cells were labeled at 4dpi, but a few labeled A cells are likely to spread the virus to other A cells via their adherens junctions within highly packed chains (Lois et al., 1996; Beier et al., 2011). We were not able to observe EGFP+ cells in the OB 28dpi. This is probably due to cell death from viral load or toxicity. Consistently, at 6dpi the number of labeled cells had decreased in the V-SVZ and RMS, and at 28dpi we did not observe virally labeled cells in these regions (data not shown).

E1 cells are another major target of supraependymal 5HT innervation in the V-SVZ. E1 cells that closely associate with supraependymal axons often contain a distinct fragment of endoplasmic reticulum cisterna with ribosomes attached on the cytoplasmic side next to the site of axonal contact, suggesting active protein synthesis at the site of interaction with the axons. Besides the lateral wall of the lateral ventricles, supraependymal axons have been observed throughout the ventricular system (Aghajanian et al., 1975; Chan-Palay, 1976; Lorez et al., 1982; Alvarez-Morujo et al., 1992). Immunostaining for AcTub on wholemounts of the medial wall of the lateral ventricles, and the walls of the third and fourth ventricles revealed similar axonal processes coursing among clusters of ependymal cilia (data not shown). Little is known about the function of these supraependymal axons. One study reported that 5HT increased the ciliary beating frequency of ependymal cells in rat brainstem slices (Nguyen et al., 2001). Supraependymal 5HT axons in the lateral ventricles might exert a similar influence on E1 cells. Consistently, our VSV(LCMV-G) transsynaptic tracing provided evidence of material exchange between dorsal raphe neurons and E1 cells of the V-SVZ, and mapping of the lateral ventricular surface revealed a distribution of supraependymal axons partially correlated with the direction of CSF flow.

Previous work using RT-PCR on dissected V-SVZ tissue suggested the expression of 5HT receptors: 1A, 1B, 1D, 2A, 2B, 2C, 3A and 6 (Councill et al., 2006) but only 1A, 2A and 2C were reported by Hitoshi et al. (2007). Dissected V-SVZ tissue is often contaminated by striatal tissue, which may explain some of the discrepancies. Here, we sorted the different V-SVZ cell populations based on marker expression prior to RT-PCR detection of 5HT receptor subtypes, minimizing contamination from adjacent tissues. We found that V-SVZ cells expressed 5HT2C and 5HT5A. Previous studies using 5HT3A-EGFP bacteria artificial chromosome (BAC) transgenic mice have shown that A cells in the RMS express 5HT3A (Inta et al., 2008). We did not detect 5HT3A in any of the sorted V-SVZ cell populations. This discrepancy might stem from different sensitivities between RT-PCR and the 5HT3A-

EGFP BAC reporter mice, or A cells might upregulate 5HT3A expression only when they leave the V-SVZ to enter the RMS.

Lesions of the raphe nuclei and administration of 5HT agonists or antagonists induce changes in adult neurogenesis, including changes in BrdU incorporation in the V-SVZ (Brezun et al., 1999; Banasr et al., 2004). Pharmacological experiments implicate the presence and functionality of 5HT1A, 5HT1B, and 5HT2C in the V-SVZ (Banasr et al., 2004, Soumier et al., 2010). However, the absence of 5HT1A and 5HT1B detected in our sorted V-SVZ cell populations suggests that these autoreceptors likely act indirectly through the dorsal raphe. It has been suggested that 5HT released by supraependymal axons activates 5HT2C in choroid plexus cells, causing them to secrete fibroblast growth factor (FGF), known to increase V-SVZ proliferation (Soumier et al., 2010). This hypothesis remains to be confirmed. However, our electrophysiology studies and acute analysis of proliferation after 5HT2C-specific drug administration, suggest that activation of 5HT2C on B1 cells could activate downstream signaling that directly promote their proliferation. Direct demonstration that regulation of neurogenesis is elicited by the 5HT axons that originate from the raphe would require electrophysiological or pharmacological stimulation of the raphe, followed by observation of altered neurogenic activity in the V-SVZ.

The dorsal raphe is known to regulate many aspects of behavior including mood, sleep, appetite, reproductive activity and cognition (Abrams et al., 2004). The role of 5HT in promoting waking and inhibiting rapid eye movement sleep (Monti et al., 2010) suggests that the dorsal raphe might exert a circadian rhythm on adult V-SVZ neurogenesis; increasing the production of OB interneurons when the animal is actively interacting with its environment and suppressing it during periods of dormant sleep. Lesion of the dorsal raphe impairs object recognition (Lieben et al., 2006), a faculty that may require the generation of new OB neurons. The dorsal raphe may also send signals through the supraependymal axons to increase V-SVZ neurogenesis during stress and anxiety, possibly anticipating a requirement for heightened olfactory function. Injection of the stress and anxiety-related neuropeptide urocortin 2 has been shown to increase c-Fos expression in 5HT neurons in the caudal part of the dorsal raphe that project to the ventricular system (Hale et al., 2010). Urocortin 1 injected into the same dorsal raphe region induces reduction in food intake (Weitemier et al., 2006). In tamoxifen-treated Nestin::CreERT2; neuron-specific enolase-diptheria toxin fragment A mice, in which newly born neurons are genetically ablated, females displayed deficits in fertility and nurturing (Sakamoto, 2010). Interestingly, a separate study shows that pregnant female mice have higher 5HT innervation in the V-SVZ (Díaz et al., 2009). Perhaps the modulation of V-SVZ neurogenesis provides a means by which the dorsal raphe influences these behavioral responses.

In sum, the present study reveals how extensive the plexus of supraependymal 5HT axons originating from the raphe nuclei is. These axons lie conspicuously on the apical surface of the lateral ventricles, a site that harbors the apical compartment of B1 cells, the largest population of NSCs in the adult brain. We demonstrate intimate contacts between B1 cells and suprependymal axons and the physiological response of these NSCs to 5HT. These findings suggest how NSCs could use a distinct network of axons, arising from nerve cells

located far away from their niche, to integrate information associated with affective control and behavior.

EXPERIMENTAL PROCEDURES

Animals

Mice were housed and treated according to the guidelines from the University of California, San Francisco (UCSF) Laboratory Animal Care and Use Committee. Wildtype CD1 mice were obtained from Harlan Laboratories. GFAP::GFP mice (FVB/N-TgGFAPGFP14Mes/J) were obtained from Jackson Laboratories. Unless otherwise stated, adult male (P30-P60) mice were used.

Tissue Preparation

Mice were deeply anesthetized with 250 mg/kg body weight tribromoethanol (Avertin) and perfused transcardially with saline (0.9% NaCl), followed by 4% paraformaldehyde (PFA). Brains were removed, post-fixed in 4% PFA at 4°C overnight, rinsed in PBS at 4°C overnight, cryoprotected in PBS/ 30% sucrose at 4°C overnight, and then cut into 50-μm sections using the sliding microtome. Coronal or sagittal sections were stored in PBS/ 0.1% sodium azide at 4°C until immun ohistochemical processing. For wholemount preparation, mice were perfused with saline. Brains were removed and the lateral walls were immediately dissected out in Leibovitz's L15 medium as previously described (Mirzadeh et al., 2008). Wholemounts were fixed in 4% PFA at 4°C overnight and then stored in PBS/ 0.1% sodium a zide at 4°C until immunohistochemical processing.

Immunohistochemistry

Both wholemounts and sections were incubated for 24–48 hours at 4°C with primary antibodies, followed by 24–48 hours at 4°C with the appropriate secondary a ntibodies (Molecular Probes, Invitrogen). The blocking solutions used were PBS/ 0.5% Triton X-100/ 10% Normal Donkey Serum (NDS) for wholemounts, and PBS / 0.1% Triton X-100/ 5% NDS for sections. For BrdU staining, samples were incubated for 40 min at 37°C w ith 2N HCl followed by 10 min at 25°C with 0.1 M boric acid (pH8.5), prior to incubation with antibodies. For mounting, the wholemounts and sections were embedded with Aqua Poly/ Mount mounting medium (Polysciences). Primary antibodies: Mouse anti-AcTub (Sigma, 1:1000), Rabbit anti-5HT (Immunostar, 1:500), Rabbit anti-SERT (Immunostar, 1:500), Rabbit anti-synaptophysin (Abcam, 1:500), Goat anti-vGluT3 (Abcam, 1:200), Rabbit anti-ACIII (Santa Cruz, 1:500), Mouse anti-β-catenin (BD Biosciences, 1:500), Chicken anti-GFP (Aves Labs, 1:500), Rabbit anti-DCX (Cell Signaling, 1:200), Mouse anti-GFAP (Millipore, 1:1000), Mouse anti-Mash1 (BD Biosciences, 1:200) and rat anti-BrdU (Abcam, 1:500).

Imaging and Quantification

High magnification images were acquired and tiled using the Leica SP5 confocal microscope. Low magnification images were acquired using the Zeiss epifluorescence microscope and tiled using the Neurolucida software (MBF Bioscience). For quantification of axon density, proportions of pinwheel cores and B1 cells associated with the axons, and

numbers of GFAP+ GFP+ cells, Mash1+ cells and DCX+ cells that co-labeled with BrdU, 4 non-overlapping high-power fields (386 × 386 μm2) in each of the 4 regions (anterior dorsal (AD), anterior ventral (AV), posterior dorsal (PD) and posterior ventral (PV)) of the lateral wall (Figure 3A) were analyzed for each hemisphere. Length of the axons was measured and double-labeled cells were counted using the Imaris software (Bitplane). For quantification of BrdU+ cells in coronal sections, high-power images of the V-SVZ were taken at 3 anterio-posterior levels (Figure S4) for each animal. Labeled cells were counted using the ImageJ software (NIH). Data were analyzed by one-way ANOVA or student's *t*-test, with a value of $P \leq 0.05$ considered statistically significant. Movie of the en-face map of supraependymal axons was constructed using the Imaris software (Bitplane).

Axon Tracing

Adult mice were anesthetized with 250 mg/kg Avertin until pedal reflex was abolished, and placed in ear bars on a stereotaxic rig. After making a small incision on the skin, a hole was drilled in the skull at the appropriate injection coordinate (see below) to expose the brain surface. The brain was injected with 250 nl of retrobeads (Lumafluor) or 10 nl of 10% BDA-10 000 (Molecular Probes, Invitrogen) from a beveled pulled glass micropipette (Wiretrol 5 ul, Drummond Scientific Company) with a 40-μm diameter tip positioned at 90° to the brain surface. The×(medial-lateral) and y (anterio-posterior) coordinates were zeroed at bregma and the z (depth) coordinate was zeroed at the brain surface (coordinates in mm). Retrobeads were injected into the lateral ventricle (x: 0.63, y: 0.38, z: −2.40) or the third ventricle (x: 0.00, y: 0.94, z: −2.40) and BDA was injected into the caudal part of the dorsal raphe (x: 0.00, y: 5.02, z: −3.50). Brains were analyzed 3 weeks post-injection. Alexa Fluor 488-streptavidin conjugate (Molecular Probes, Invitrogen) was used to visualize the BDA. For transsynaptic tracing, 250 nl of 7.2 × 10^8 transduction unit per ml VSV(LCMV-G) (from Dr. Leszek Lisowski, GT3 Core Facility, Salk Institute) were stereotactically injected into the dorsal raphe (x: 0.00, y: 5.02, z: −3.50). Control injections were made by injecting 30 nl of the virus at every 0.50-mm depth interval at the coordinates (x: 00, y: 5.02, z: −0.50 to −3.00). Injected brains were analyzed at 1, 2, 3, 4, 5, 6 and 28dpi.

Electron Microscopy

For TEM, mice were anesthetized as described above (see Tissue Preparation) and perfused with 2% PFA/2.5% glutaraldehyde. Brains were removed, post-fixed in 2% PFA/ 2.5% glutaraldehyde overnight, rinsed in 0.1 M PB, and cut into 200-μm sections using the vibratome. Sections were post-fixed in 2% osmium, dehydrated, and embedded in Araldite (Durcupan, Fluka). Semithin sections (1.5 μm) were cut with a diamond knife and stained with 1% toluidine blue for light microscopy. Ultrathin sections (70 nm) were cut, stained with lead citrate, and examined under a TEM (Tecnai Spirit G2, FEI, Oregon) using a digital camera (Morada, Soft Imaging System, Olympus, Japan). For pre-embedding immunogold stainings, mice were perfused with 4% PFA/ 0.5% glutaraldehyde. Brains were post-fixed in 4% PFA and cut into 50-μm sections using the vibratome. Pre-embedding immunogold stainings were carried out as previously described (Sirerol-Piquer et al, 2012). Sections were contrasted with 1% osmium/ 7% glucose and embedded in araldite. 1.5-μm semithin sections were prepared, selected at the light microscope level, and cut into 70-nm ultrathin sections.

Pharmacological Studies

Miniosmotic pumps (Alzet 1007D) were assembled under sterile conditions, filled with vehicle (saline), fenfluramine (200 μg/ml) (Sigma), RO600175 (400 μg/ml) (Tocris Bioscience) or SB206553 (160 μg/ml) (Sigma) and allowed to equilibrate at 37°C overnigh t. Pump implantation was performed on a stereotaxic rig as previously described (Ihrie et al., 2011), such that the cannula was inserted into the lateral ventricle (x: 1.10, y: 0.00, z: −2.35). Mice with fenfluramine pumps were analyzed 2 days post-implantation and mice with RO600175 or SB206553 pumps were analyzed 5 days post-implantation. For acute agonist and antagonist treatment, 500 nl of saline, RO600175 (400 μg/ml) or SB206553 (160 μg/ml) was injected into the lateral ventricle (x: 0.63, y: 0.38, z: −2.40) as described above (see Axon Tracing). V-SVZ wholemounts were dissected from the contralateral hemispheres 4 hours post-injection. The mice were injected I.P. with 50 mg/kg BrdU 1 hour before perfusion.

FACS and RT-PCR

V-SVZ were dissected from adult GFAP::GFP mice or wildtype CD1 mice and cut into small pieces with a hand-held scalpel in cold L15 medium. Papain (Worthington) was activated in 1.1 mM EDTA / 5.5 mM cysteine HCl for 30 min and mixed with L15 medium to a 6 mg/ml solution and sterile filtered. Tissue was incubated in papain solution for 10 min at 37°C, spun down at 13 00 rpm for 5 min at 4°C, resuspended in 10% FBS / 0.5 mg/ml DNAse in Neurobasal medium and pipette-triturated. Dissociated cells were laid on top of cold 22% Percoll (Sigma), spun down at 1800 rpm for 30 min at 4°C and resuspended in 1% BSA / 0.1% glucose in HBSS. Cells were simultaneously incubated for 30 min with phycoerythrin (PE)-conjugated rat anti-CD24 (BD Pharmingen, 1:100) and biotinylated EGF coupled with Alexa Fluor 647-streptavidin (EGFA647) (Molecular Probes, Invitrogen, 1:300) (Pastrana et al., 2009). All of the different cell populations were isolated in one single sort using a Becton Dickinson FACS Aria II (BD Biosciences) using 13 psi pressure and 100-μm nozzle aperture. Data were collected by using a linear digital signal process. Gates were set manually using control samples (Figure S5). Data were analyzed with FlowJo software. Sorted cells were collected in RLT lysis buffer and stored at −80°C until all samples were collecte d. RNA isolation was done with the RNeasy Plus Micro kit (QIAGEN). cDNA was synthesized using SuperScript III RT (Invitrogen) and RT-PCR was completed using SYBR Green PCR Master Mix (Applied BioSystems) on an ABI7900HT.

Electrophysiology

V-SVZ wholemounts were dissected from GFAP::GFP mice (P7-12). Patch electrodes were made from borosilicate glass capillaries (B-120-69-15, Sutter Instruments) with a resistance of 5–7 MΩ. Pipettes were tip-filled with internal solution containing (in mM): 125 K-gluconate, 15 KCl, 10 HEPES, 4 MgCl2, 4 Na2ATP, 0.3 Na3GTP, 10 Tris-phosphocreatine, 0.2 EGTA. Individual wholemounts were transferred to a submerged recording chamber and continuously perfused with oxygenated (95% O2 and 5% CO2) artificial CSF (aCSF) containing (in mM): 125 NaCl, 2.5 KCl, 2 CaCl2, 1.3 MgCl2, 1.3 NaH2PO4, 25 NaHCO3, 10 glucose. (4.0 ml/min) at 30–32°C. Slices were visualized under a microscope (Olympus BX50WI) using infrared video microscopy and differential interference contrast optics.

Recordings were made with an Axon 700B patchclamp amplifier and 1320A interface (Axon Instruments). Signals were filtered at 2 kHz using amplifier circuitry, sampled at 10 kHz, and analyzed using Clampex 10.2 (Axon Instruments). For local drug application, drugs were pressure applied through a pipette (tip diameter 10–20 μm) to the established whole-cell patches. All antagonists were bath applied.

Supplementary Material

Refer to Web version on PubMed Central for supplementary material.

Acknowledgments

We thank all members of the Alvarez-Buylla laboratory for helpful discussions. Special thanks to Michael Kissner for FACS technical support, Kenneth X. Probst for the illustration in the Graphical Abstract, and Luis C. Fuentealba and Thuhien Nguyen for critical reading of the manuscript. This work is funded by the US National Institutes of Health (NS29978 and HD23901). A.A.-B. is the Heather and Melanie Muss Endowed Chair of Neurological Surgery at UCSF. C.K.T. is supported by the Singapore Agency for Science, Technology and Research. J.D.C. is a recipient of the CARE & CURE Pediatric Epilepsy Fellowship from Epilepsy Foundation of Greater Los Angeles.

REFERENCES

Abrams JK, Johnson PL, Hollis JH, Lowry CA. Anatomic and functional topography of the dorsal raphe nucleus. Ann NY Acad Sci. 2004; 1018:46–57. [PubMed: 15240351]

Aghajanian GK, Gallager DW. Raphe origin of serotonergic nerves terminating in the cerebral ventricles. Brain Res. 1975; 88:221–231. [PubMed: 167906]

Alvarez-Morujo AJ, Toranzo D, Blázquez JL, Peláez B, Sánchez A, Pastor FE, Amat G, Amat P. The ependymal surface of the fourth ventricle of the rat: a combined scanning and transmission electron microscopic study. Histol Histopathol. 1992; 7:259–266. [PubMed: 1515709]

Arrant AE, Jemal H, Kuhn CM. Adolescent male rats are less sensitive than adults to the anxiogenic and serotonin-releasing effects of fenfluramine. Neuropharmacology. 2013; 65:213–222. [PubMed: 23103347]

Banasr M, Hery M, Printemps R, Daszuta A. Serotonin-induced increases in adult cell proliferation and neurogenesis are mediated through different and common 5-HT receptor subtypes in the dentate gyrus and the subventricular zone. Neuropsychopharmacology. 2004; 29:450–460. [PubMed: 14872203]

Beier T, Saunders A, Oldenburg IA, Miyamichi K, Akhtar N, Luo L, Whelan SP, Sabatini B, Cepko CL. Anterograde or retrograde transsynaptic labeling of CNS neurons with vesicular stomatitis virus vectors. Proc Natl Acad Sci USA. 2011; 109:9219–9219.

Bonsi P, Cuomo D, Ding J, Sciamanna G, Ulrich S, Tscherter A, Bernardi G, Surmeier DJ, Pisani A. Endogenous serotonin excites striatal cholinergic interneurons via the activation of 5-HT 2C, 5-HT6, and 5-HT7 serotonin receptors: implications for extrapyramidal side effects of serotonin reuptake inhibitors. Neuropsychopharmacology. 2007; 32:1840–1854. [PubMed: 17203014]

Brezun JM, Daszuta A. Depletion in serotonin decreases neurogenesis in the dentate gyrus and subventricular zone of adult rats. Neuroscience. 1999; 89:999–1002. [PubMed: 10362289]

Chan-palay V. Serotonin axons in the supra- and subependymal plexuses and the leptomeninges; their roles in local alterations of the cerebrospinal fluid and vasomotor activity. Brain Res. 1976; 102:103–130. [PubMed: 813816]

Councill JH, Tucker ES, Haskell GT, Maynard TM, Meechan DW, Hamer RM, Lieberman JA, LaMantia AS. Limited influence of olanzapine on adult forebrain neural precursors in vitro. Neuroscience. 2006; 140:111–122. [PubMed: 16564641]

Díaz D, Valero J, Airado C, Baltanás FC, Weruaga E, Alonso JR. Sexual dimorphic stages affect both proliferation and serotonergic innervation in the adult rostral migratory stream. Exp Neurol. 2009; 216:357–364. [PubMed: 19162010]

Dinopoulos A, Dori I. The development of the serotonergic fiber network of the lateral ventricles of the rat brain: a light and electron microscopic immunocytochemical analysis. Exp Neurol. 1995; 133:73–84. [PubMed: 7601265]

Doetsch F, Alvarez-Buylla A. Network of tangential pathways for neuronal migration in adult mammalian brain. Proc Natl Acad Sci USA. 1996; 93:14895–14900. [PubMed: 8962152]

Doetsch F, Caillé I, Lim DA, García-Verdugo JM, Alvarez-Buylla A. Subventricular zone astrocytes are neural stem cells in the adult mammalian brain. Cell. 1999; 97:703–716. [PubMed: 10380923]

Fu W, Le Maître E, Fabre V, Bernard JF, David Xu ZQ, Hökfelt T. Chemical neuroanatomy of the dorsal raphe nucleus and adjacent structures of the mouse brain. J Comp Neurol. 2010; 518:3464–3494. [PubMed: 20589909]

Fuentealba LC, Obernier K, Alvarez-Buylla A. Adult neural stem cells bridge their niche. Cell Stem Cell. 2012; 10:698–708. [PubMed: 22704510]

Hale MW, Stamper CE, Staub DR, Christopher A. Urocortin 2 increases c-Fos expression in serotonergic neurons projecting to the ventricular/periventricular system. Exp Neurol. 2010; 224:271–281. [PubMed: 20382145]

Hitoshi S, Maruta N, Higashi M, Kumar A, Kato N, Ikenaka K. Antidepressant drugs reverse the loss of adult neural stem cells following chronic stress. J Neurosci Res. 2007; 85:3574–3585. [PubMed: 17668856]

Hornung JP. The human raphe nuclei and the serotonergic system. J Chem Neuroanat. 2003; 26:331–343. [PubMed: 14729135]

Ihrie RA, Shah JK, Harwell CC, Levine JH, Guinto CD, Lezameta M, Kriegstein AR, Alvarez-Buylla A. Persistent sonic hedgehog signaling in adult brain determines neural stem cell positional identity. Neuron. 2011; 71:250–262. [PubMed: 21791285]

Inta D, Alfonso J, von Engelhardt J, Kreuzberg MM, Meyer AH, van Hooft JA, Monyer H. Neurogenesis and widespread forebrain migration of distinct GABAergic neurons from the postnatal subventricular zone. Proc Natl Acad Sci USA. 2008; 105:20994–20999. [PubMed: 19095802]

Jahanshahi A, Temel Y, Lim LW, Hoogland G, Steinbusch HW. Close communication between the subependymal serotonergic plexus and the neurogenic subventricular zone. J Chem Neuroanat. 2011; 42:297–303. [PubMed: 21924347]

Kriegstein A, Alvarez-Buylla A. The glial nature of embryonic and adult neural stem cells. Ann Rev of Neurosci. 2009; 32:149–184. [PubMed: 19555289]

Lacar B, Young SZ, Platel JC, Bordey A. Imaging and recording subventricular zone progenitor cells in live tissue of postnatal mice. Front Neurosci. 2010; 4:1–16. [PubMed: 20582256]

Lieben CKJ, Steinbusch HW, Blokland A. 5,7-DHT lesion of the dorsal raphe nuclei impairs object recognition but not affective behavior and corticosterone response to stressor in the rat. Behav Brain Res. 2006; 168:197–207. [PubMed: 16360222]

Liu X, Bolteus AJ, Balkin DM, Henschel O, Bordey A. GFAP-Expressing Cells in the Postnatal Subventricular Zone Display a Unique Glial Phenotype Intermediate Between Radial Glia and Astrocytes. Glia. 2006; 410:394–410. [PubMed: 16886203]

Lledo PM, Merkle FT, Alvarez-Buylla A. Origin and function of olfactory bulb interneuron diversity. Trends Neurosci. 2008; 31:392–400. [PubMed: 18603310]

Lois C, García-Verdugo JM, Alvarez-Buylla A. Chain migration of neuronal precursors. Science. 1996; 271:978–981. [PubMed: 8584933]

Lorez HP, Richards JG. Supra-ependymal serotoninergic nerves in mammalian brain: morphological, pharmacological and functional studies. Brain Res. 1982; 9:727–741.

Mathew TC. Association between supraependymal nerve fibres and the ependymal cilia of the mammalian brain. Anat Histol Embryol. 1999; 28:193–197. [PubMed: 10458025]

Merkle FT, Tramontin AD, García-Verdugo JM, Alvarez-Buylla A. Radial glia give rise to adult neural stem cells in the subventricular zone. Proc Natl Acad Sci USA. 2004; 101:17528–17532. [PubMed: 15574494]

Mirzadeh Z, Merkle FT, Soriano-Navarro M, García-Verdugo JM, Alvarez-Buylla A. Neural stem cells confer unique pinwheel architecture to the ventricular surface in neurogenic regions of the adult brain. Cell Stem Cell. 2008; 3:265–278. [PubMed: 18786414]

Monti JM. The role of dorsal raphe nucleus serotonergic and non-serotonergic neurons, and of their receptors, in regulating waking and rapid eye movement (REM) sleep. Sleep Med Rev. 2010; 14:319–327. [PubMed: 20153670]

Nguyen T, Chin WC, O'Brien JA, Verdugo P, Berger AJ. Intracellular pathways regulating ciliary beating of rat brain ependymal cells. J Physiol. 2001; 531:131–140. [PubMed: 11179397]

Pastrana E, Cheng LC, Doetsch F. Simultaneous prospective purification of adult subventricular zone neural stem cells and their progeny. Proc Natl Acad Sci USA. 2009; 106:6387–6392. [PubMed: 19332781]

Ponti G, Obernier K, Guinto C, Jose L, Bonfanti L, Alvarez-Buylla A. Cell cycle and lineage progression of neural progenitors in the ventricular-subventricular zones of adult mice. Proc Natl Acad Sci USA. 2013; 110:E1045–E1054. [PubMed: 23431204]

Sakamoto M, Imayoshi I, Ohtsuka T, Yamaguchi M, Mori K, Kageyama R. Continuous neurogenesis in the adult forebrain is required for innate olfactory responses. Proc Natl Acad Sci USA. 2011; 108:8479–8484. [PubMed: 21536899]

Sawamoto K, Wichterle H, Gonzalez-Perez O, Cholfin JA, Yamada M, Spassky N, Murcia NS, García-Verdugo JM, Marin O, Rubenstein JL, et al. New neurons follow the flow of cerebrospinal fluid in the adult brain. Science. 2006; 311:629–632. [PubMed: 16410488]

Shen Q, Wang Y, Kokovay E, Lin G, Chuang SM, Goderie SK, Roysam B, Temple S. Adult SVZ stem cells lie in a vascular niche: a quantitative analysis of niche cell-cell interactions. Cell Stem Cell. 2008; 3:289–300. [PubMed: 18786416]

Sirerol-Piquer MS, Cebrián-Silla A, Alfaro-Cervelló C, Gomez-Pinedo U, Soriano-Navarro M, García-Verdugo JM. GFP immunogold staining, from light to electron microscopy, in mammalian cells. Micron. 2012; 43:589–599. [PubMed: 22227011]

Soumier A, Banasr M, Goff LK, Daszuta A. Region- and phase- dependent effects of 5-HT(1A) and 5-HT(2C) receptor activation on adult neurogenesis. Eur Neuropsychopharmacol. 2010; 20:336–345. [PubMed: 20022222]

Tavazoie M, Van der Veken L, Silva-Vargas V, Louissaint M, Colonna L, Zaidi B, García-Verdugo JM, Doetsch F. A specialized vascular niche for adult neural stem cells. Cell Stem Cell. 2008; 3:279–288. [PubMed: 18786415]

Tong CK, Alvarez-Buylla A. SnapShot: Adult Neurogenesis in the V-SVZ. Neuron. 2014; 81:220. [PubMed: 24411739]

Weitemier AZ, Ryabinin AE. Urocortin 1 in the dorsal raphe regulates food and fluid consumption, but not ethanol preference in C57BL/6J mice. Neuroscience. 2006; 137:1439–1445. [PubMed: 16338088]

Young SZ, Taylor MM, Bordey A. Neurotransmitters couple brain activity to subventricular zone neurogenesis. Eur J Neurosci. 2012; 33:1123–1132. [PubMed: 21395856]

HIGHLIGHTS

- Supraependymal serotonergic axons blanket the apical surface of V-SVZ
- Supraependymal axons make intimate contacts with a subpopulation of B1 cells
- 5HT2C contributes to the serotonergic axonal control of the adult stem cell niche

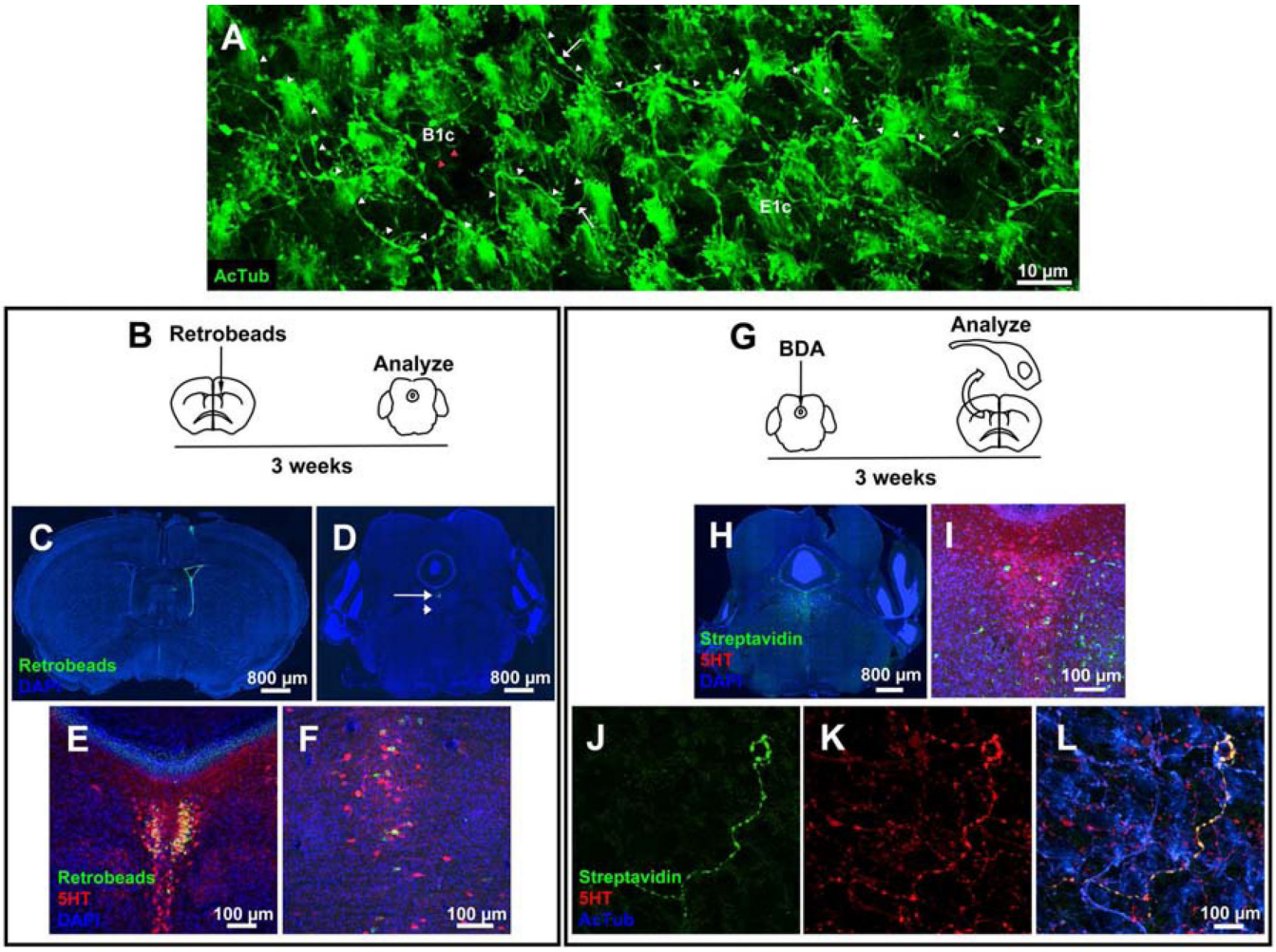

Figure 1. Supraependymal axons in the lateral ventricles originate from dorsal and median raphe nuclei

(A) En-face view of V-SVZ stained with antibodies against AcTub show in addition to the motile cilia in E1 cells (E1c) and primary cilia of B1 cells (B1c, red arrowheads), long fibers (white arrowheads) with varicosities (arrows) corresponding to the supraependymal axons. (B) 3 weeks after injection of retrobeads into the lateral ventricle (C), cell bodies in the raphe nuclei (dorsal (arrow in D, magnified in E) and median (arrowhead in D, magnified in F)) are labeled. Retrobeads are present in a subpopulation of raphe nuclei cell bodies that express 5HT (E–F). For a sagittal view see Figure S1. (G) BDA injected into the dorsal raphe (H, magnified in I) is transported anterogradely into the walls of the lateral ventricle where it is present in a subpopulation of supraependymal 5HT axons (J–L).

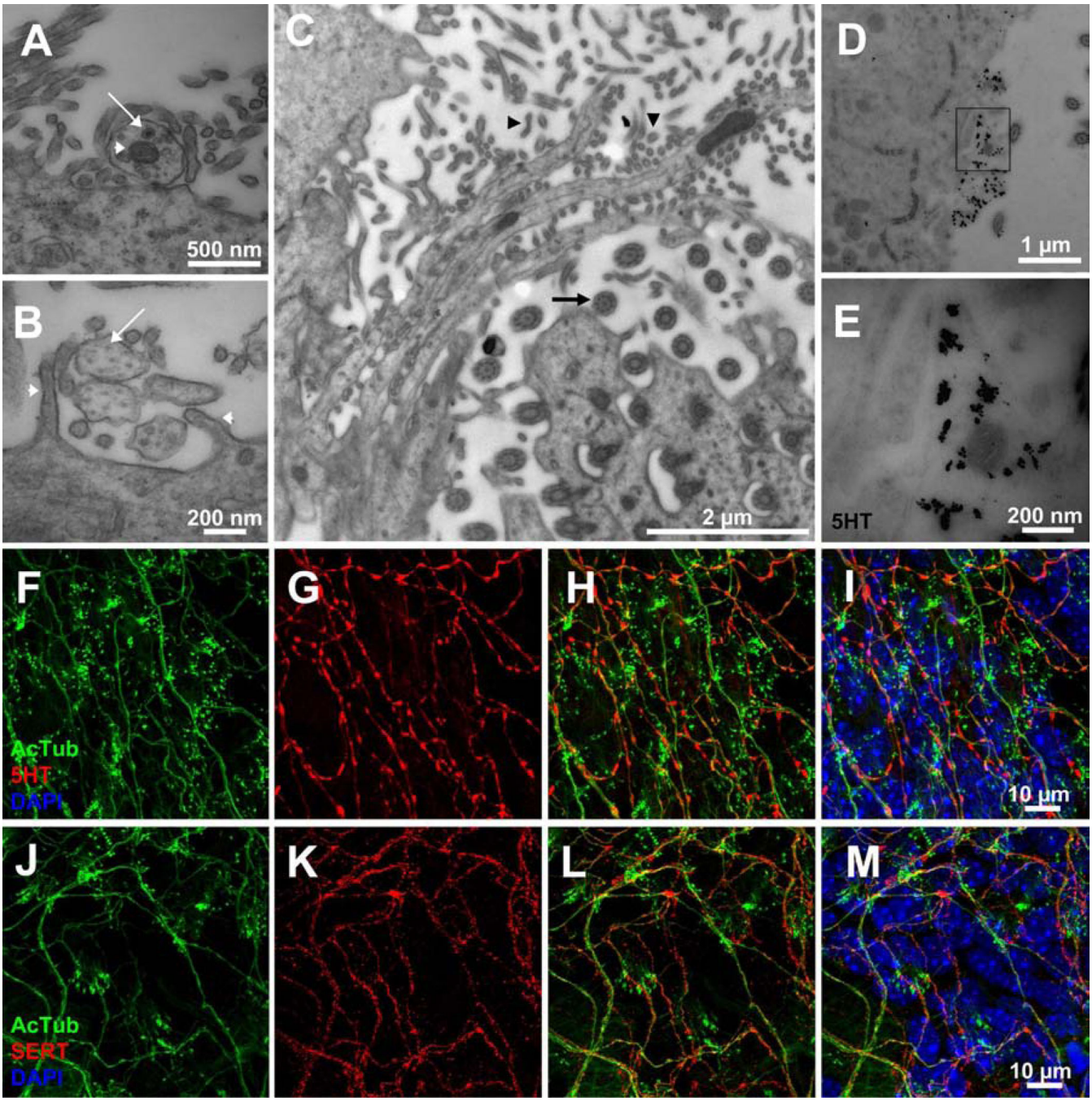

Figure 2. Supraependymal axons are serotonergic and tightly bound to the ependymal surface by microvilli

(A) TEM shows that supraependymal projections have characteristic features of unmyelinated axons. Note the presence of vesicles (arrow) and mitochondria (arrowhead). (B) Cross-section of microtubules (arrow) oriented parallel to the axon shafts. Note how microvilli (arrowheads) “hug” the axons. (C) Tangential view of the ventricular wall showing the alignment of microvilli (arrowheads) along single and bundled supraependymal axons. Note how the axons circumvent ependymal cilia (arrow). (D–E) Immunogold staining for 5HT confirms supraependymal axons are serotonergic. (F–I) Confocal

microscopy showing co-staining of 5HT in AcTub+ supraependymal axons. (J–M) AcTub+ supraependymal axons also co-express SERT.

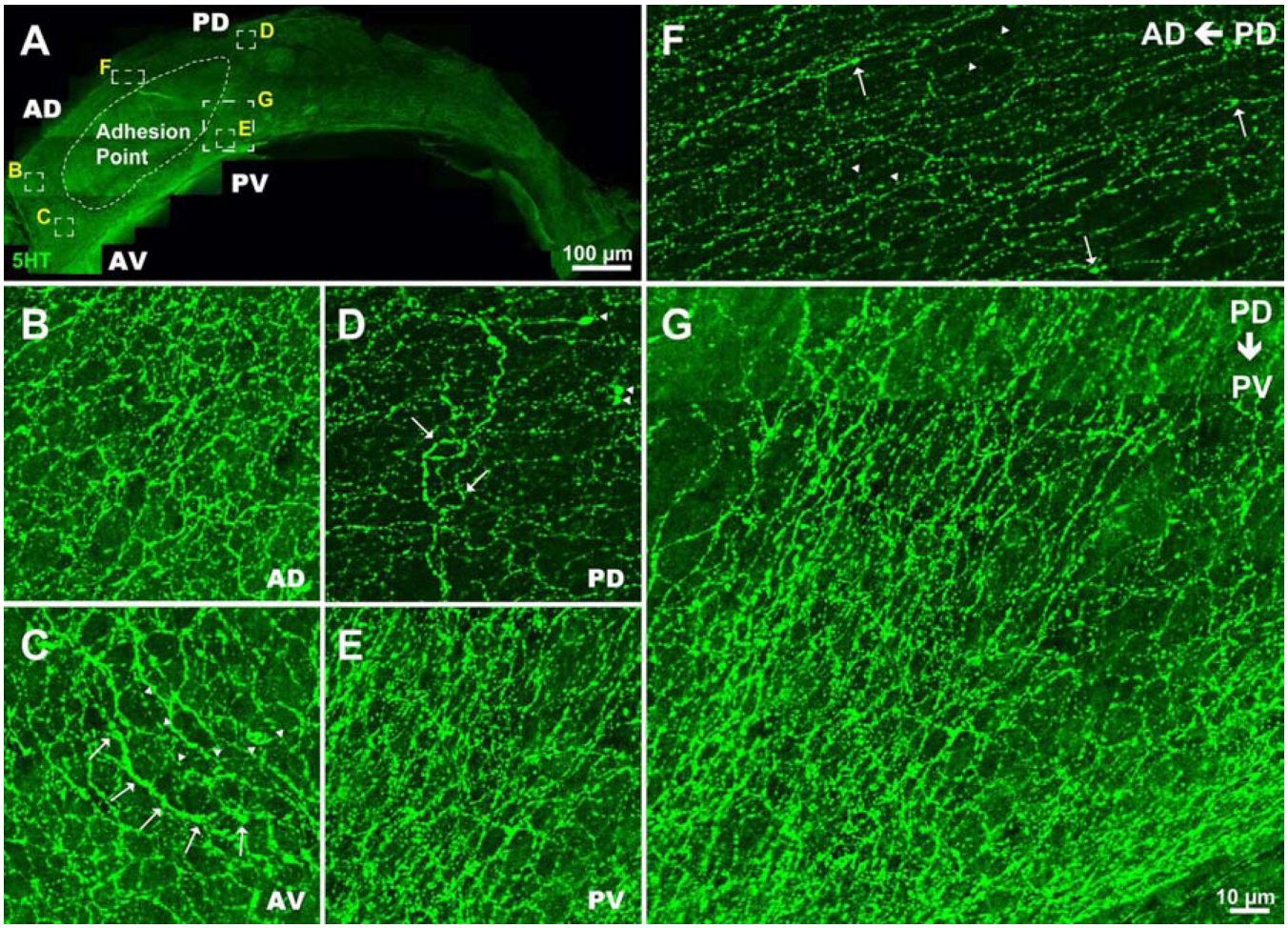

Figure 3. Supraependymal 5HT axons are densely present throughout most of the lateral wall of the lateral ventricle

(A–E) Dense axons are present in the anterior dorsal (AD), anterior ventral (AV), posterior dorsal (PD) and posterior ventral (PV) regions of the V-SVZ. For a panoramic view see Movie S1. Many supraependymal axons run parallel to the anterio-posterior axis of the lateral ventricle, an orientation similar to that of CSF flow and neuroblast migration (Sawamoto et al., 2006); note orientation of axons dorsal (F) and posterior (G) to the adhesion point. (C) Arrows and arrowheads point to thick and thin axons, respectively. (D) Arrows and arrowheads indicate loops and bulbous structures, respectively. (F) Large and small varicosities (arrows and arrowheads, respectively) are present along the axons giving the impression of beaded threads. For axon densities at different developmental ages see Figure S2.

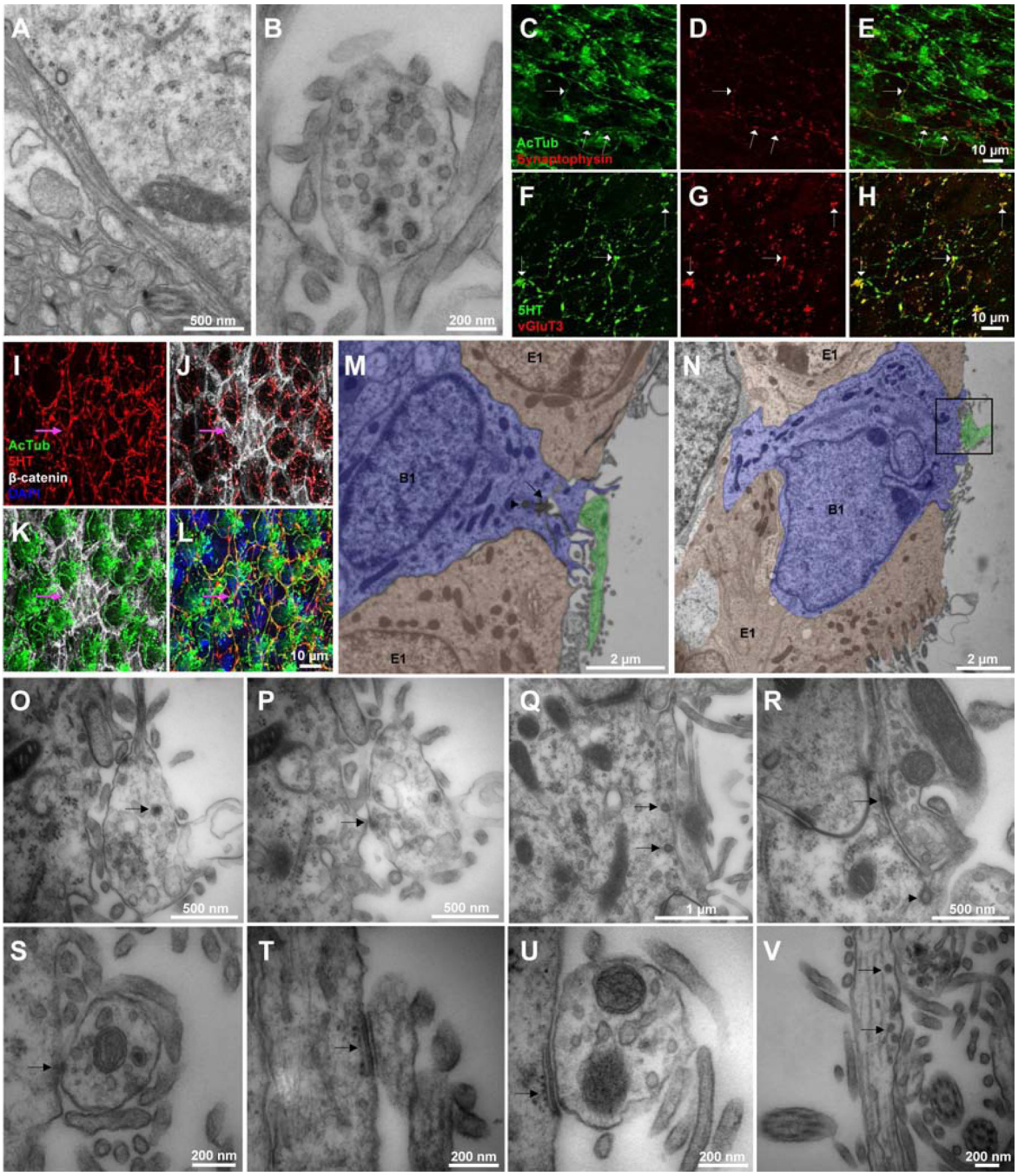

Figure 4. Varicosities in supraependymal axons contain synaptic markers and vesicles, and they make specialized contacts with B1 and E1 cells

En-face (A) and transverse (B) views of supraependymal axons show light and dark-core vesicles in the varicosities. The varicosities also contain the presynaptic markers synaptophysin (C–E, arrows) and vGluT3 (F–H, arrows). (I–L) Supraependymal axons criss-cross pinwheels and have varicosities at their cores where B1 cells' apical endings are located. Arrow indicates a cluster of 7 B1 cells. (M–N) Pseudo-colored TEM images showing endings of supraependymal axons on the apical surface of B1 cells. (M) Arrow and arrowhead point to primary cilia and an orthogonal sister centriole, respectively. (O–P) High

magnification serial sections of boxed region in panel N (see Figure S3 for complete series of sections). (O) Arrow points to dark-core vesicle within the axon terminal. (P, R) Electrondense profiles (arrow) indicative of specialized contacts between supraependymal axons and B1 cells could be observed. (Q) Arrows indicate clathrin-coated vesicles forming on a B1 cell membrane next to a supraependymal axon. (R) Arrowhead points to complementary membrane invaginations on a B1 cell and an adjacent supraependymal axon. (S) Supraependymal axons also form desmosome-like contacts with a putative E1 cell. (T–U) A piece of endoplasmic reticulum cisterna is often observed adjacent to the site of contact. (V) Membrane invaginations and clathrin-coated vesicles also occur in the supraependymal axons.

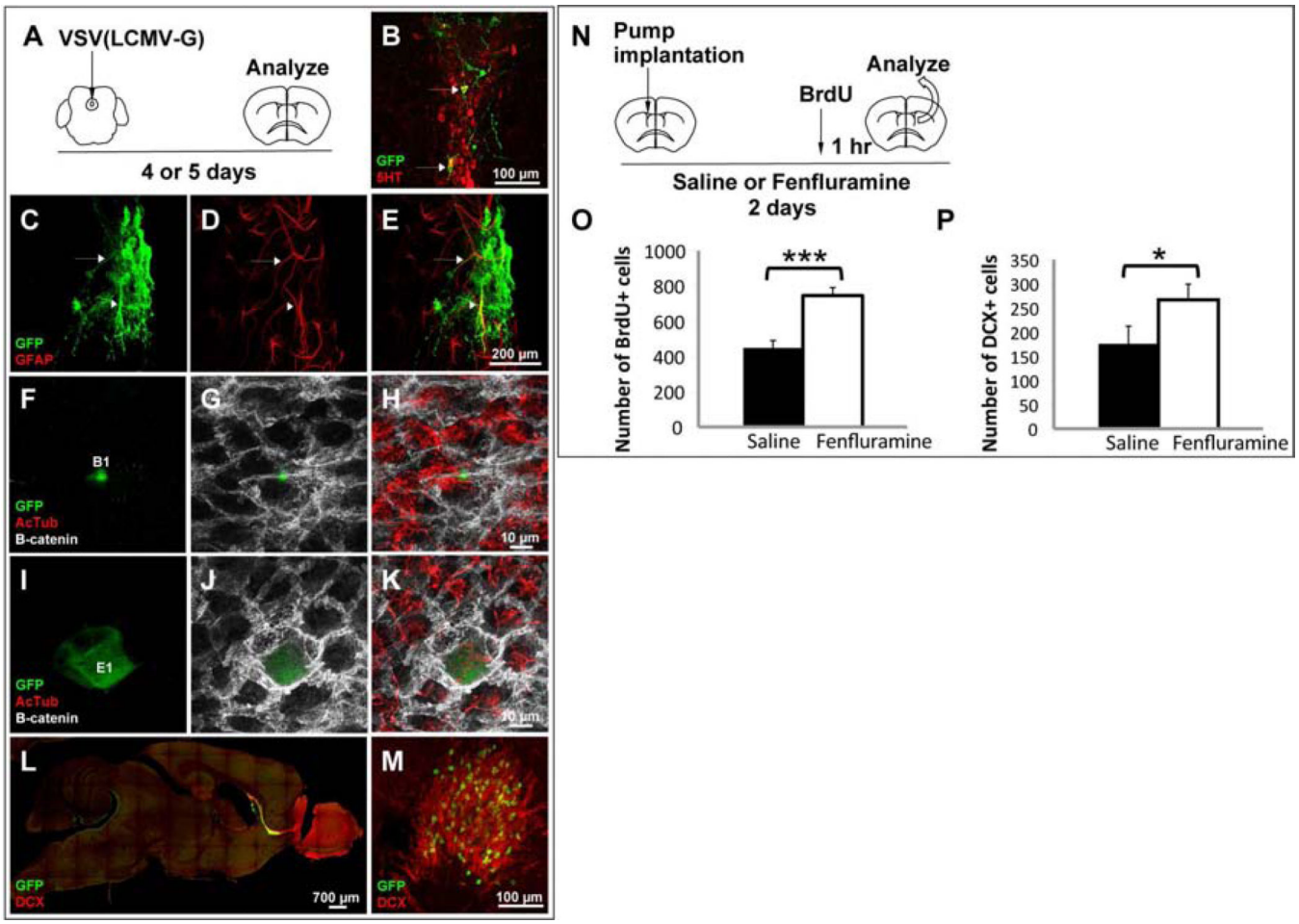

Figure 5. Transsynaptic VSV(LCMV-G) injected into the dorsal raphe spreads into V-SVZ cells. Fenfluramine-induced 5HT release increases proliferation and neurogenesis in the V-SVZ

(A) 4 or 5 days after VSV(LCMV-G) injection into the dorsal raphe nucleus, a small number of infected 5HT neurons is observed at the site of injection (arrows in B). The virus is also present in B1 cells of the V-SVZ: coronal section (C–E, for orthogonal projections of regions indicated by arrow and arrowhead, see Figure S4B and C, respectively) and wholemount preparation (F–H). (I–K) A small number of virally labeled E1 cells are also EGFP+. (L–M) EGFP is also observed in A cells migrating along the RMS in sagittal (L) and coronal (M) sections. (N) Fenfluramine was infused into the lateral ventricle by miniosmotic pump for 2 days. (O–P) Quantification of BrdU+ cells (O) and DCX+ cells (P) shows significant increase in proliferation and neurogenesis following fenfluramine administration. *** $P < 0.002$ * $P < 0.05$ from student's *t*-test. Error bars = s.d. from at least three mice per experimental group. See Figure S4 for immunohistochemistry data.

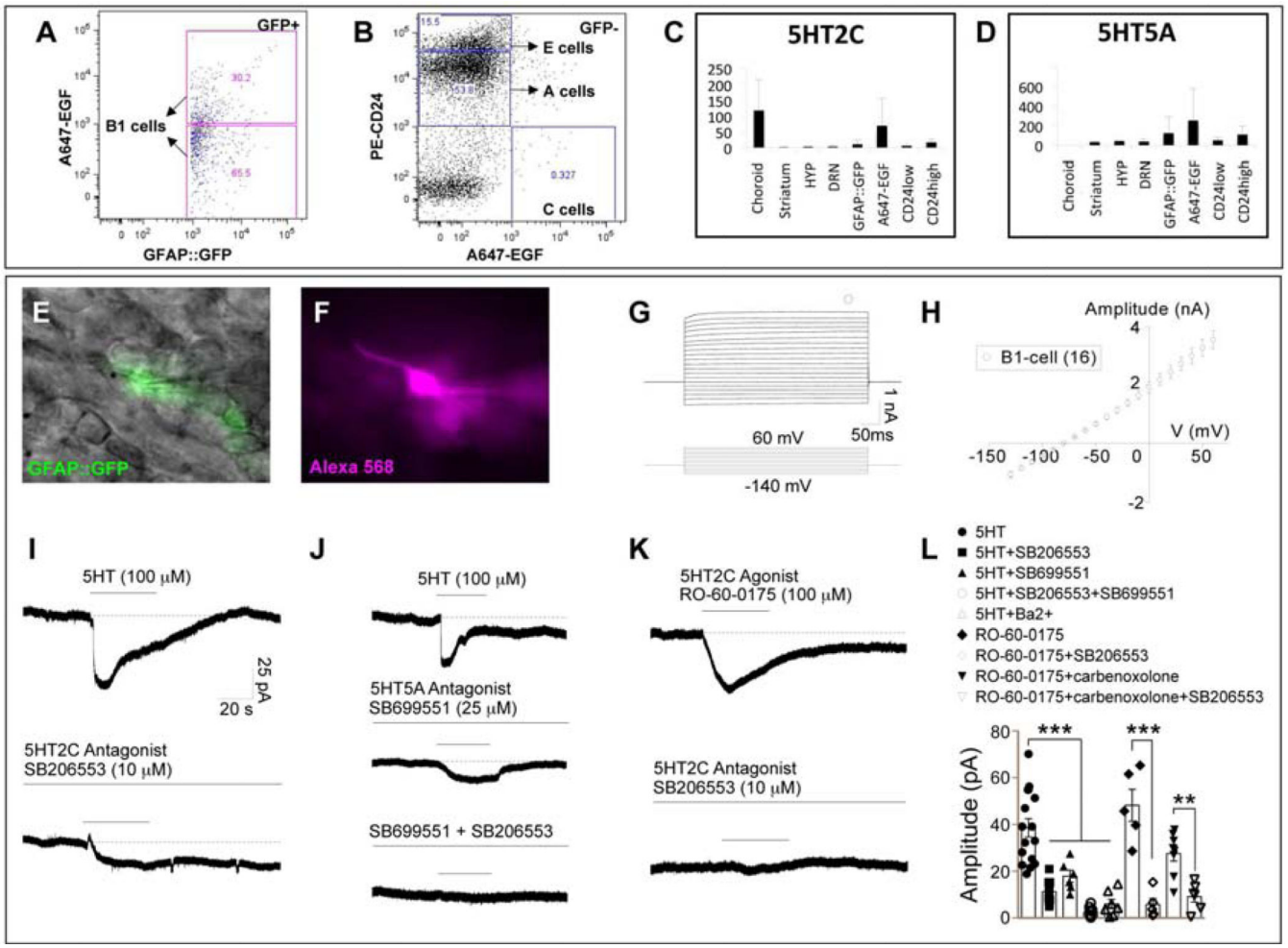

Figure 6. B1 cells express 5HT receptors 2C and 5A

(A–B) A combination of expression of EGFR, CD24 and GFAP::GFP in transgenic mice was used to sort for B1 cells (GFP+), C cells (GFP− EGFR+ CD24−), A cells (GFP− EGFR − CD24low) and E1 cells (GFP− EGFR− CD24high) as previously described in Pastrana et al. (2009) (see Figure S5 for FACS controls). (C–D) Out of the 12 5HT receptor subtypes tested, only 2C and 5A are detected in V-SVZ cells by RT-PCR. HYP; hypothalamus, DRN; dorsal raphe nucleus. Error bars = s.d. from three independent experiments (see Figure S5 for RT-PCR data of other receptor subtypes). (E–L) V-SVZ wholemounts dissected from GFAP::GFP mice were used for patch-clamp recording of B1 cells. (E) Differential interference contrast (DIC) image superimposed with GFP fluorescence (green). (F) B1 cells were also identified by their cell morphology as shown by intracellular loading with Alexa Fluor 568 (magenta); note the long process extending from the cell body. (G) Representative traces showing whole-cell currents of B1 cells upon stepped potentials ranging from −140 mV to 60 mV at a holding potential of −80 mV. (H) I–V curve of B1 cells. (I–J) B1 cells display inward currents in response to local application of 5HT. This current is partially blocked in the presence of 5HT2C antagonist (SB206553) (I, bottom) or 5HT5A antagonist (SB699551) (J, middle). (J, bottom) Co-application of 5HT2C antagonist and 5HT5A antagonist completely abolishes the 5HT-induced current. (K) Inward current induced by

5HT2C agonist (RO-60-0175) is also completely inhibited by 5HT2C antagonist. (L) Bar graph showing 5HT-induced currents in the absence or presence of 5HT2C and/or 5HT5A antagonist(s) or Ba2+, and 5HT2C agonist-induced currents in the absence or presence of 5HT2C antagonist and/or the gap junction blocker carbenoxolone. ***P < 0.001 **P < 0.01 from student's *t*-test or one-way ANOVA with post hoc bonferroni test. Error bars = S.E.M.

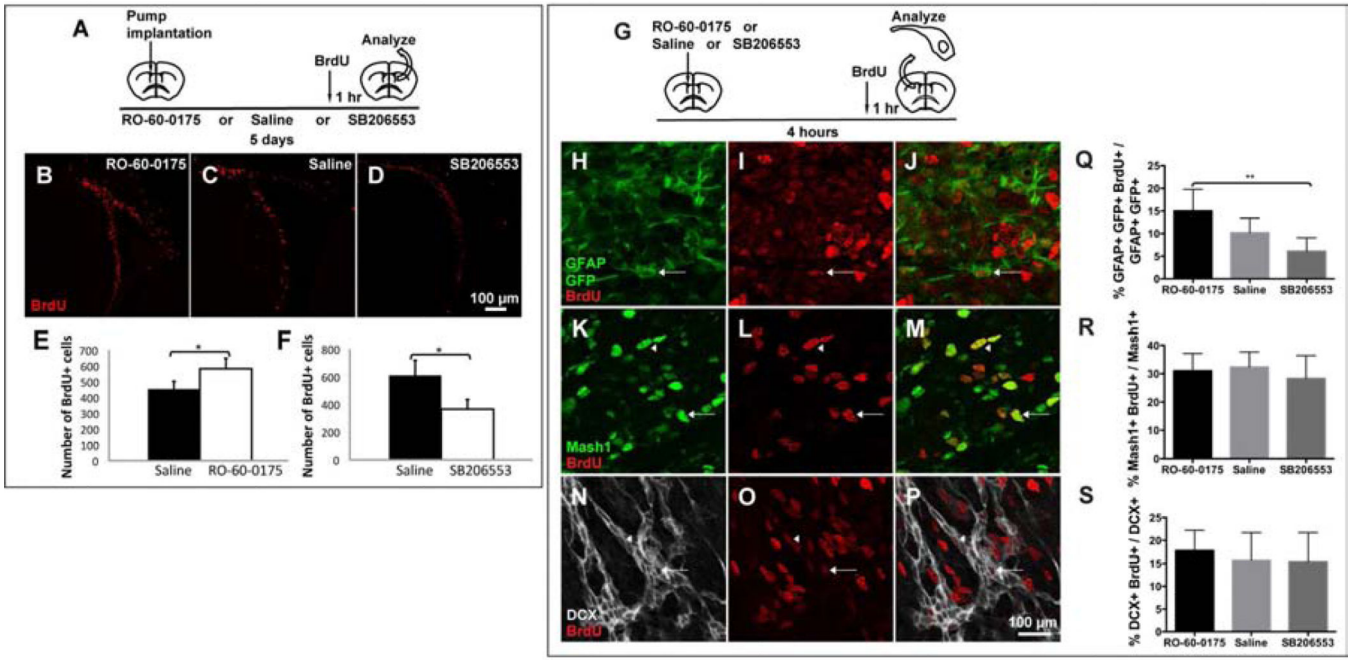

Figure 7. 5HT2C agonist increases V-SVZ B1 cell proliferation and antagonist decreases it

(A) 5-day infusion of 5HT2C agonist and antagonist results in increased (B, E) and decreased (D, F) numbers of BrdU+ cells, respectively, in the V-SVZ compared to saline-infused controls (C). * $P < 0.05$ from student's *t*-test. Error bars = s.d. from at least three mice per experimental group. (G) For cell population analysis of proliferation, adult GFAP::GFP mice or wild type CD1 mice were injected intraventricularly with 5HT2C agonist or antagonist and their V-SVZ were dissected from the contralateral hemisphere 4 hours post-injection. (H–P) The V-SVZ whole mounts were stained for GFAP/GFP (B1 cell marker) (H–J), Mash1 (C cell marker) (K–M) and DCX (A cell marker) (N–P). Cells co-labeled with BrdU are indicated by arrows. (Q–S) Bar graphs showing the proliferating fractions of B1 (Q), C (R) and A (S) cells in agonist and antagonist-treated mice. **$P < 0.02$ from one-way ANOVA with post hoc Turkey test. Error bars = S.E.M. from at least five mice per experimental group. For total numbers of BrdU+, B1, C and A cells, see Figure S6.